



ACADEMIC
PRESS

Available online at www.sciencedirect.com

SCIENCE @ DIRECT®

NeuroImage

NeuroImage 20 (2003) 1468–1484

www.elsevier.com/locate/ynimg

Geometric atlas: modeling the cortex as an organized surface

Roberto Toro* and Yves Burnod¹

Inserm Unité 483. Université Pierre et Marie Curie 9, quai Saint-Bernard, 75005 Paris, France

Received 10 December 2002; revised 14 July 2003; accepted 21 July 2003

Abstract

Recent atlases of the cortical surface are based on a modelization of the cerebral cortex as a topological sphere. This captures effectively its organization as a regular bidimensional sheet of layers parallel to the surface and with perpendicular cortical columns. Yet, while in the vertical direction cortices are almost the same throughout phyla, in the sense of its surface the cerebral cortex is one of the most variable and distinctive parts of the nervous system. Indeed, gyri and sulci appear to have a crucial organizing role in an architectonic, connective, and functional sense. This organization is not explicitly captured by the surface model of the cortex. We propose a geometric model of the cortical anatomy based on flat representations of principal sulci obtained from surface reconstructions of MRI data, and on neuroanatomical and theoretical considerations concerning the folding patterns of the cortex. The cortex is modeled by a sphere where primary sulci are included as axes. The arrangement of the axes is a simplification of the arrangement of principal sulci observed in flat stereographic representations of the whole cortical surface. The position of secondary and tertiary sulci is then defined by a field of orientations parallel and orthogonal to the axes. We consider the use of the geometric model as a synthetic reference cortex for addressing reconstructions of cortical surfaces. We present a method which establishes a bijection between the geometric model and a cortical surface reconstruction by using the axes of the model as boundary conditions for a set of partial differential equations solved over both surfaces. Using the geometric model as atlas provides a natural parameterization of the cortical surface that, unlike angular coordinates, allows for a localization based on the surface distance to its main organizing landmarks and folding patterns.

© 2003 Elsevier Inc. All rights reserved.

1. Introduction

1.1. The cortex as a surface

The concept of the cerebral cortex as a surface is of great importance in understanding its many topologically organized maps. Retinotopy, ocular dominance bands, tonotopy, and somatotopy cannot be properly grasped if they are not considered within the appropriate two-dimensional metric.

The concern with the bidimensional character of the cerebral cortex is particularly relevant in human brain mapping, where most of the contemporary work is done in a three-dimensional framework: the stereotaxic space of Talairach and Tournoux (1988). In this coordinate system, the points of the brain are associated with three normalized

coordinates related to the AC-PC line. The brain structures are thus described in relation to the corpus callosum, a stable reference landmark. Applied to the cerebral cortex, this method is imprecise (Fischl et al., 1999b). It is frequent indeed that coordinates supposed to refer to the cortex will actually address noncortical structures. Conceptually more important, the euclidean distance between two points risks to subevaluate the actual distance over the cortical surface. The lack of an explicit definition of the structure of the cerebral cortex is at the origin of these problems.

The cerebral cortex is comparable to a highly folded two-dimensional sheet differentiated in an almost fixed number of layers. In the sense perpendicular to the surface, these layers are physiologically and anatomically arranged in cortical columns. Physiologically, all the neurons in the same columns have similar functional properties, for example, similar receptive fields in the case of the primary somatosensory (Mountcastle, 1957) and visual (Hubel and Wiesel, 1977) cortices. Anatomically, staining the cortical

* Corresponding author.

E-mail address: rtoro@snv.jussieu.fr (R. Toro).

¹ E-mail address: ybteam@ccr.jussieu.fr (Y. Burnod).

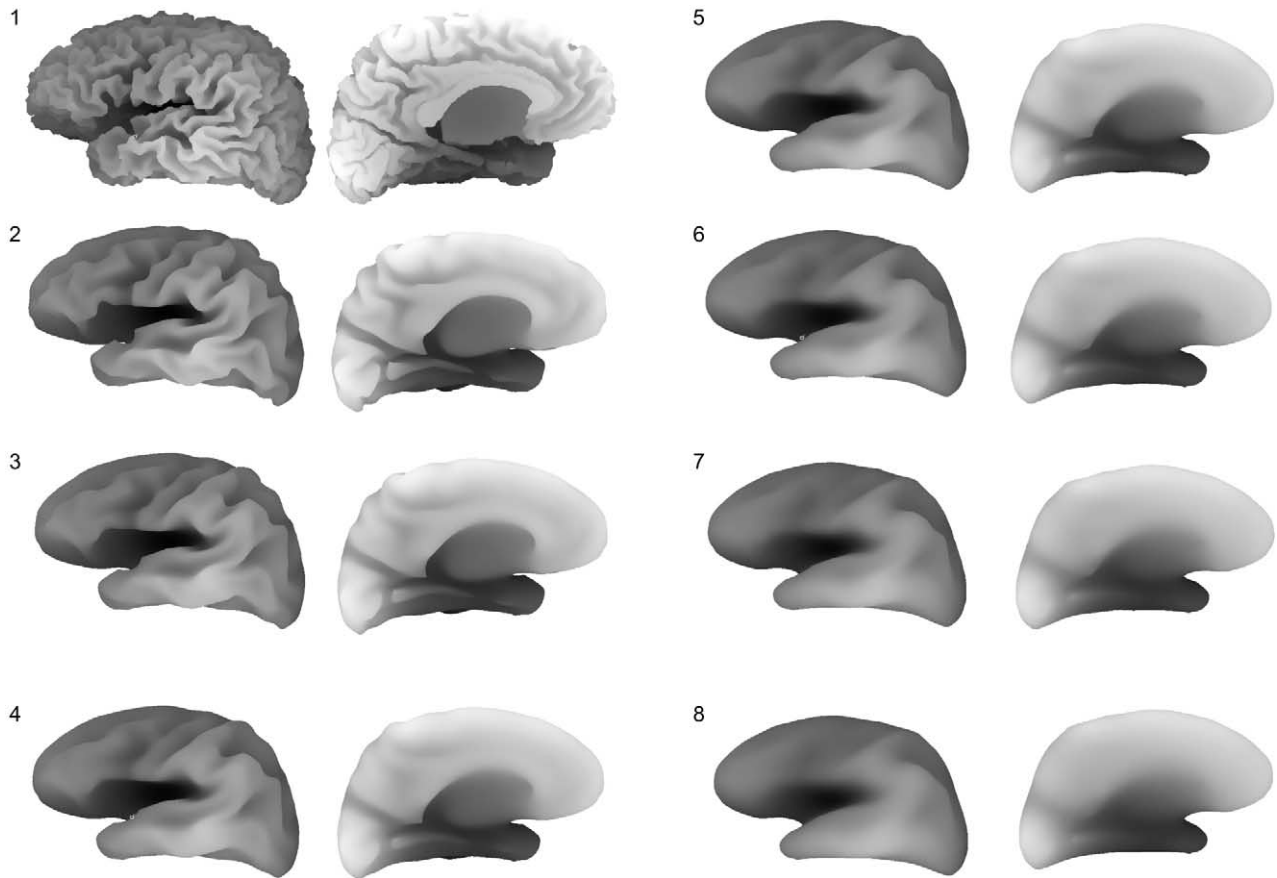


Fig. 1. Sulcal depth throughout the iterative smoothing. The iterative smoothing of a reconstructed cortical surface produces the successive fading of tertiary, secondary, and finally primary sulci. The figure illustrates some steps in the iteration of the algorithm that transforms each point of a reconstructed surface into the average of its neighbors. Iteration steps are respectively 0, 100, 200, 300, 400, 500, 600, and 800. Gray levels are a representation of the sulcal depth.

afferent fibers has revealed this columnar structure as a widespread organizational principle of the cortical architecture (Mountcastle, 1957; 1997; Hubel and Wiesel, 1977; Goldman and Nauta, 1977). These cortical columns are not isolated elements; they are profusely interconnected in the horizontal direction (Valverde, 1986). All these anatomic-functional considerations support the widely accepted computational concept of the cortex as a bidimensional mosaic of interrelated columnar modules (Mountcastle, 1978, 1997). The layered and columnar structure is in fact a fundamental characteristic of the cortex that can be traced back to its ontogeny (Marin-Padilla, 1988; Rakic, 1988).

This regular structure of the cortical surface is well captured by modeling the surface of a cerebral hemisphere as topologically equivalent to a sphere (Dale and Sereno, 1993; Thompson and Toga, 1997; Van Essen and Drury, 1997; Van Essen et al., 1998; Dale et al., 1999; Fischl et al., 1999a). The surface topology allows an easy definition of a normal vector for the columnar organization, and a tangent plane for the orientation of the cortical layers that is also the plane for the horizontal columnar connectivity. A surface

reconstruction of the cortical surface from a three-dimensional matrix of anatomical data can capture its topology in a way consistent with its ontogeny.

1.2. The cortex as an organized surface

Many fundamental processes of the cortical development, however, will disrupt this initial regular structure. At the end of cell migration from the ventricular plate, synaptic development (Armstrong et al., 1995), neuronal differentiation and dendrogenesis (Welker, 1990), cortical lamination (Smart and McSherry, 1986a, 1986b), and development of thalamo-cortical and cortico-cortical connections (Goldman and Galkin, 1978; Goldman-Rakic, 1980) all mark the beginning of cortical fissuration in most large brain mammals. The result is the architectonic, connectional, and functional differentiation of the cortex in gyri and sulci arranged in folding patterns characteristic of a given species (Welker, 1990; Nieuwenhuys et al., 1997). In the human brain, the cortical folds have been classified as primary, secondary, and tertiary according to its time of development, degree of

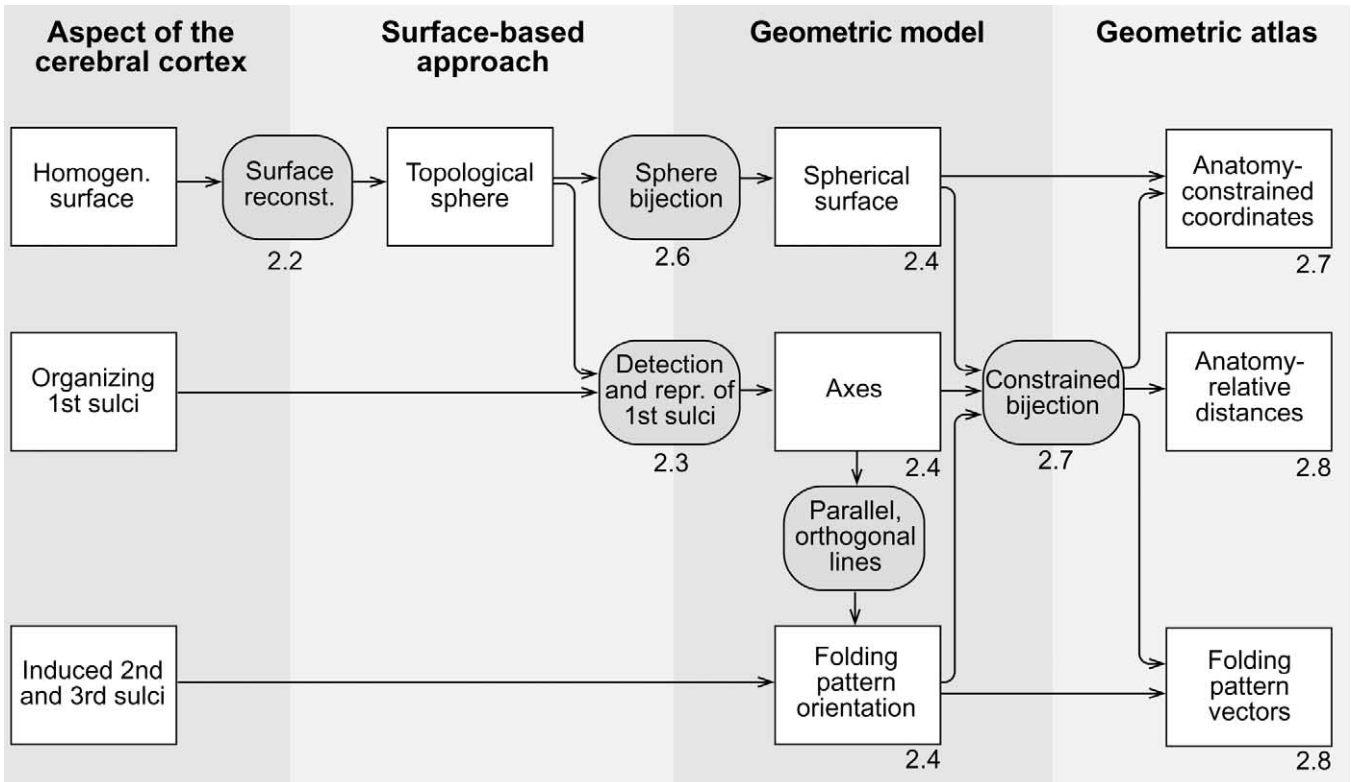


Fig. 2. Overview. Concepts introduced and related models, methods, and applications.

variability, and depth (Jacobson, 1991; Armstrong et al., 1995; Connolly, 1950; Bailey and von Bonin, 1950). Primary sulci are quite invariant, while secondary sulci show more individual variation and tertiary sulci are very variable. Primary sulci appear to have constant relations to cytoarchitecture, a relation that is less clear for secondary and tertiary sulci (Zilles et al., 1997; Roland and Zilles, 1998; Morosan et al., 2001; Hasnain et al., 2001). Finally, primary sulci are also deeper than secondary, and the latter deeper than tertiary, which can be seen from the progressive smoothing of a surface reconstruction of the cortex (Fig. 1).

In the same manner that the stereotaxic space of Talairach does not define explicitly the structure of the cortex, the surface-based approaches do not define explicitly the anatomical organization of the cortex. In the same way that stereotaxic coordinates do not make any distinction, and refer all the points of the brain—cortical or non cortical—to the same landmark (the AC-PC line), spherical coordinates do not allow any distinction of the points of the cortical surface in relation to the main gyri and sulci, and refer them to an abstract point: the origin of the angular coordinates system.

1.3. Geometric model and atlas

Making explicit the anatomical organization of the cortex is a complicated task, mainly because of its great vari-

ability: even the principal sulci change their shape from one hemisphere to the other in the same individual (Ono et al., 1990; Damasio, 1995). However, there appears to be some regularities that make possible the definition of a basic pattern of distribution of gyri and sulci over the cortex. As has been observed by neuroanatomists (Malamud and Hirano, 1974; Welker, 1990; Ono et al., 1990), the folding patterns of the medial surface of the hemispheres seem to be influenced by the development of the corpus callosum. The congenital absence of this structure is associated with the absence of a parallel cingulate gyrus and the disruption of the general radial folding pattern of the medial surface. In fact, it can be observed that many principal sulci seem to have the same influence in its surrounding folding pattern. For example (and as can be also seen in Fig. 1), parallel secondary sulci appear at both sides of the central sulcus (the pre- and postcentral sulci) and of the calcarine sulcus. Furthermore, the superior and inferior opercula can be seen as gyri parallel to the insula.

Based on their studies of the human sulcal anatomy Régis et al. (2003) have proposed the parallel and orthogonal distribution of convolutions as a fundamental principle of their organization. This pattern is much more clear in mammals such as canids, where the sylvian fissure is often surrounded by parallel ectosylvian and supra sylvian sulci. Todd (1982, 1985) has proposed a geometric model for the folding patterns based on this simpler anatomy. It suggests

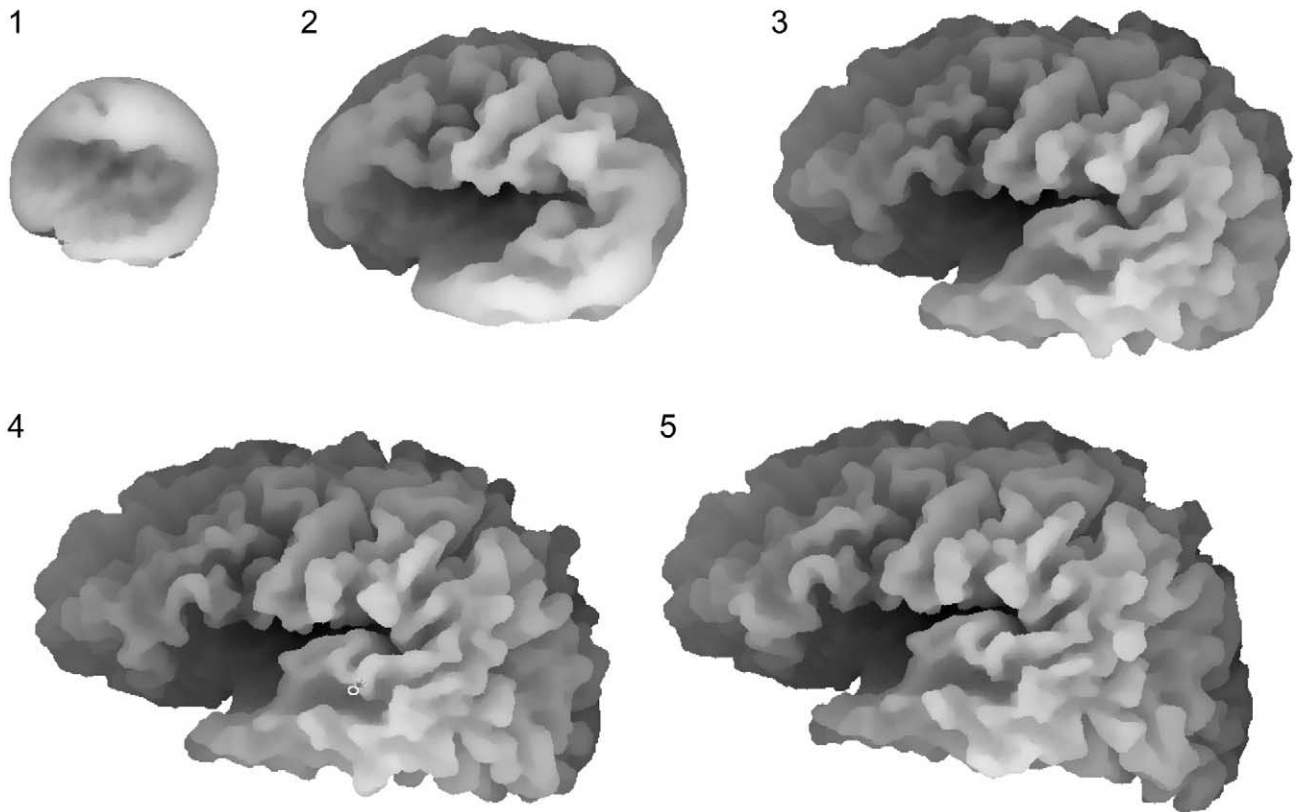


Fig. 3. Reconstruction of the cortical surface. A topologically spherical reconstruction of the cortical surface is obtained by the progressive expansion of an initially small deformable surface. The deformable surface is described both as a vectorial mesh and as a voxel surface, which allows the surface to grow many times its initial size without self-intersections and without strong smoothing constraints. The initial surface (not shown in the figure) consists of 8 points and 12 triangles, while the final surface is in the order of 150.000 points and 300.000 triangles. The steps 50, 100, 150, 200, 300 and 400 of the procedure are shown.

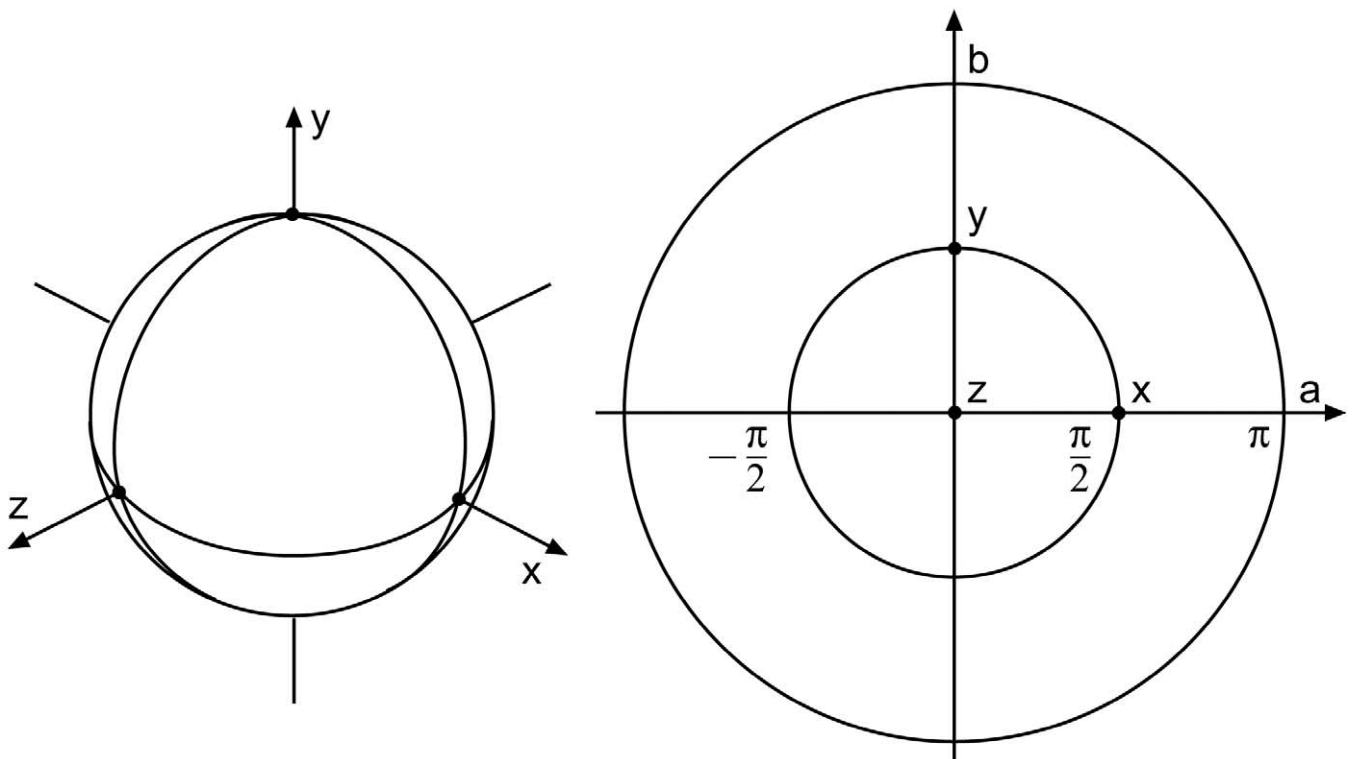


Fig. 4. Polar stereographic projection. The z pole of the sphere (left) is at the center of the polar stereographic projection (right). The sphere is opened at the $-z$ pole that becomes the external circle of the polar stereographic projection.

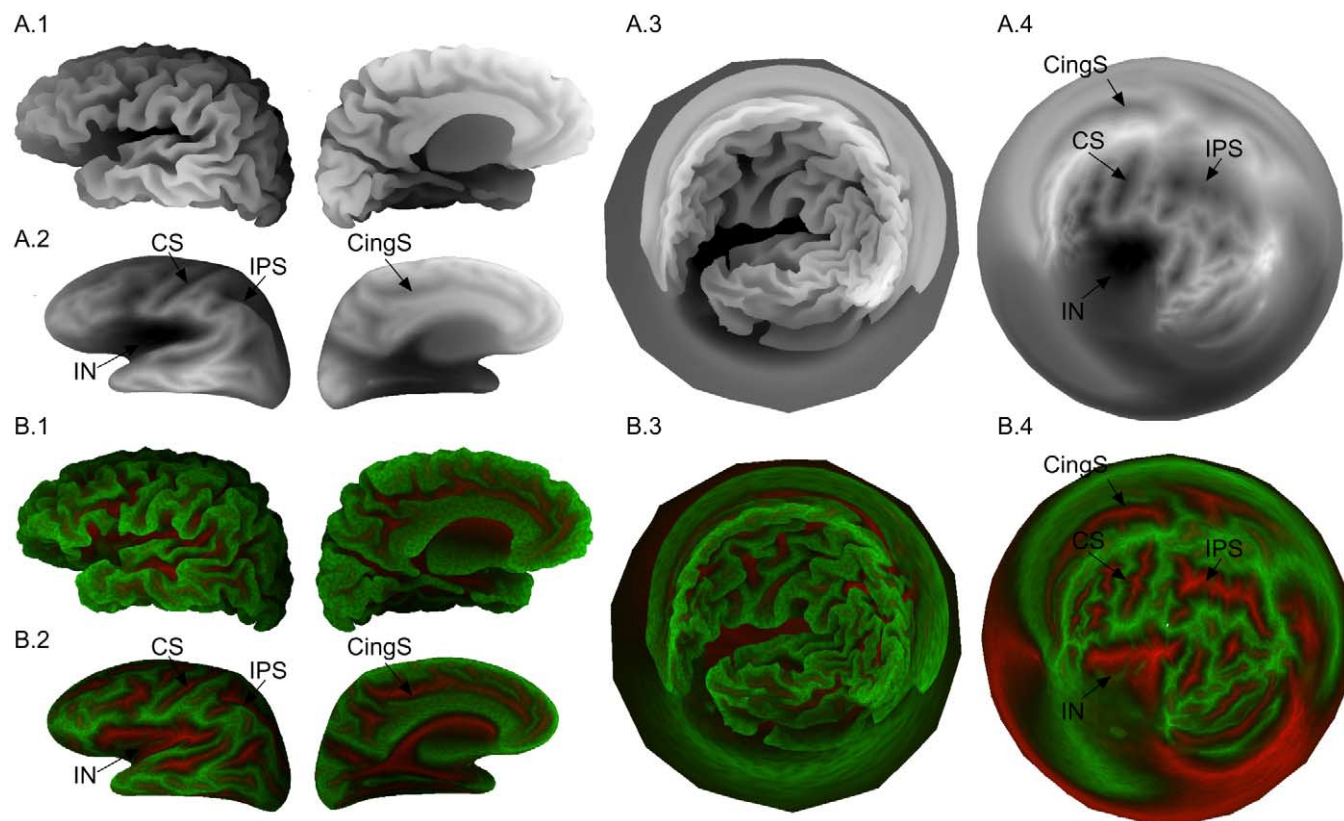


Fig. 5. Mapping of the sulcal depth and integrated curvature patterns. (Top images) The sulcal depth evaluated as the distance between the surface and a bounding ellipsoid mapped in levels of gray. The mapping of the sulcal depth gives a hierarchical image of the cortical anatomy where deeper landmarks are easily distinguishable. From left to right: temporal and medial images of the mapping of the sulcal depth over (A.1) a reconstructed surface, (A.2) a smoothed surface, (A.3) stereographic representations of the reconstruction and (A.4) its spherical projection. The stereographic representation of the spheric projection of a reconstructed surface is a flat disk that shows the whole cortical surface. (Bottom images) The integration of the mean curvature patterns through smoothing steps. Concavity is represented in levels of red, convexity in levels of green, and inflexion in black. The mapping of the integrated curvature patterns allows an easy distinction of the most persistent gyri and sulci by hierarchically weighting the classical mean curvature representation. From left to right: temporal and medial images of the mapping of the integrated curvature patterns over (B.1) a reconstructed surface, (B.2) a smoothed surface, (B.3) stereographic representations of the reconstruction, and (B.4) its spheric projection.

that the cortex folds along the orthogonal system formed by the principal lines of curvature of the surface, in accordance with a principle of “minimal radial distortion.” This principle states that transverse motion, or slipping, of the cortical surface during convolution development will be disfavored by the mechanical action of the radial glial and neuronal fibers. Thus the folds will follow the directions of minimal curvature, which minimize the slipping (Todd, 1982).

In this paper we propose a new *geometric model* for the organization of the human cortical surface based on the following hypotheses: (i) the cerebral cortex can be modeled as a topological sphere, (ii) over its surface, a set of principal sulci induce a folding pattern field, and (iii) further secondary and tertiary gyri and sulci will be oriented along this field parallel to, and orthogonal to, the principal sulci. In the geometric model, the cortex is represented by a sphere where principal sulci are included as axes over its surface. The arrangement of the axes is a simplification of the arrangement of principal sulci and other important anatom-

ical landmarks as they are observed in flat stereographic representations of the whole cortical surface. The position of secondary and tertiary sulci is then modeled as small circles and geodesics with orientations parallel and orthogonal to the axes.

Next, we consider the use of the geometric model as synthetic reference cortex for addressing reconstructions of cortical surfaces. We call this atlas the *geometric atlas*. Current surface-based atlases of the cortical surface use reconstructed cortices as reference (Toga and Thompson, 2001). In different approaches this can be an arbitrary consensual cortex (one of the Visible Human Project cortices, for example (Spitzer et al., 1996; Van Essen and Drury, 1997; Van Essen et al., 1998)), or an average cortex computed from a set of surface reconstructions (Fischl et al., 1999b; Thompson et al., 1996). While in both approaches the structure of the cerebral cortex is made explicit (it is equivalent to a sphere), this is not the case for the structure of its principal sulci and folding patterns. In the geometric

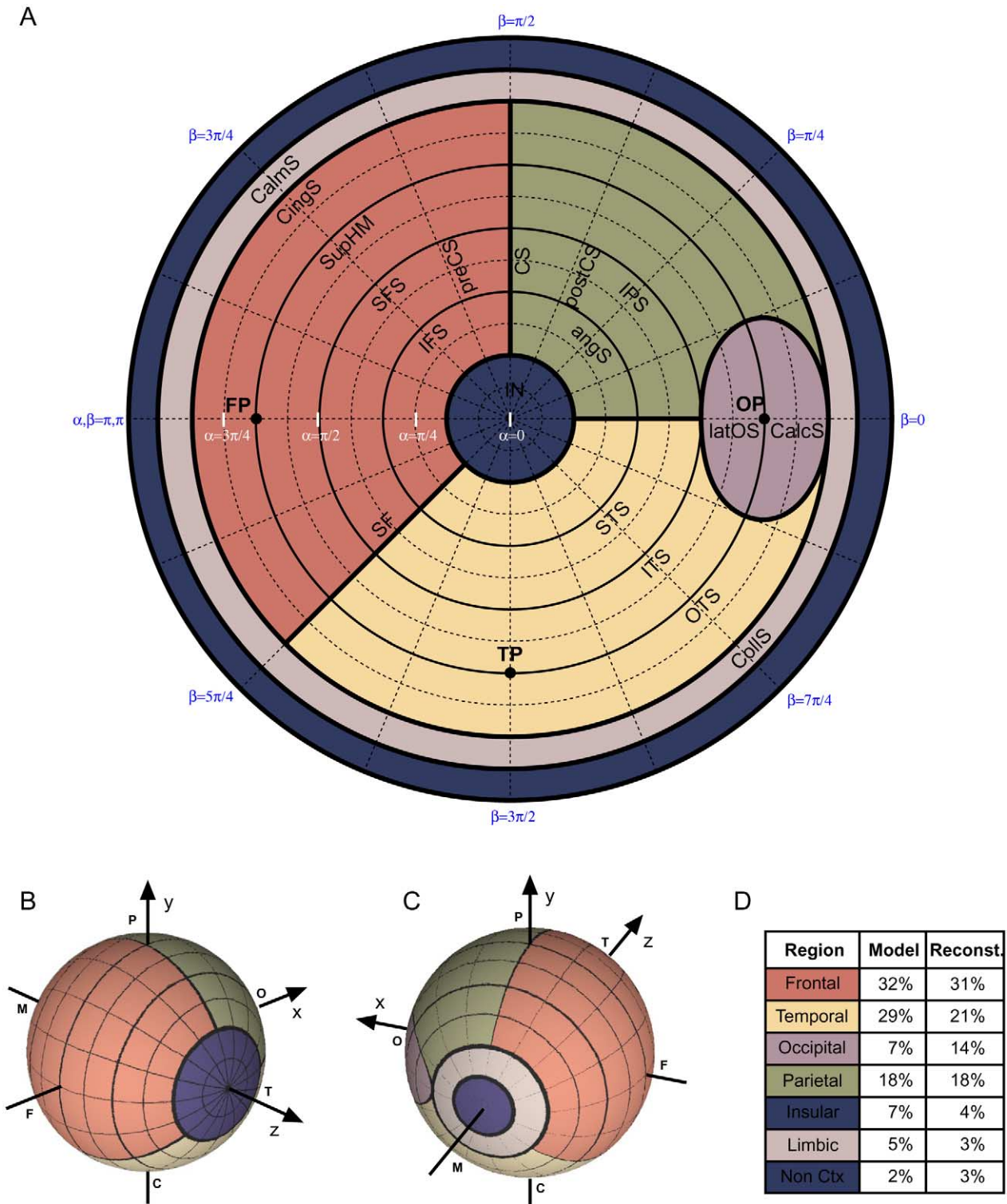


Fig. 6. Geometric model. (A) Stereographic representation and (B,C) two three-dimensional images of the axes, folding pattern, and regions of the geometric model. Table D compares the proportions of the cortical regions in the geometric model and in surface reconstructions. The frontal lobe region is represented in red, parietal lobe region in green, occipital lobe region in violet, temporal lobe region in yellow, limbic lobe region in gray, and insular and noncortical region in blue. The positions for the frontal pole (FP), temporal pole (TP) and occipital pole (OP) are indicated by a point. Heavy lines indicate the axes of the model, associated to the central sulcus (CS), callosomarginal sulcus (CalmS), calcarine sulcus (CalcS), collateral sulcus (CollS), and other important landmarks as the Insula (IN), Sylvian fissure (SF), and superior hemisphere margin (SupHM). Continuous lines and dotted lines represent the induced folding pattern, and some sulci nomenclature is indicated: small circles concentric to the insula and the callosomarginal sulcus, cingulate sulcus (CingS), superior and inferior frontal sulci (SFS, IFS), superior and inferior temporal sulci (STS, ITS), occipitotemporal sulcus (OTS), angular sulcus (angS), and intraparietal sulcus (IPS). In the geodesics orthogonal to the insula and the callosomarginal sulcus: pre- and postcentral sulci (preCS, postCS) and lateral occipital sulcus (latOS).

atlas the surface and the organization are represented by the geometric model, providing a common basic pattern for overlaying further data. The mapping between the geometric model and a cortical reconstruction is established using the axes of the geometric model as boundary conditions for a set of partial differential equations (PDE) solved over the surfaces (Chung, 2001; Haker et al., 2000). In this way, we are able to provide a strict correspondence between the axes of the geometric model, and an adaptive projection of its folding patterns.

Once the mapping between geometric model and reconstructed cortical surface has been established, the cortical surface is parameterized by a coordinate system whose constant lines globally follow the principal orientations of the cortical convolutions. We call these coordinates *anatomy-constrained angular coordinates*. All the points of the cortical surface can be addressed by this coordinate system and we can also obtain two vectors for its two principal orientations in the folding pattern field (parallel to, and orthogonal to, the curves of the insula and the callosomarginal sulcus). The anatomical landmarks represented by the axes of the geometric model have constant reference positions, which allows us to measure the surface-distance between a given point of the surface and the set of axes along the lines of the anatomy-constrained angular coordinates. We call these the *anatomy-relative distances*. As pure angular coordinates, anatomy-constrained angular coordinates address the cortex as a two-dimensional surface. Unlike pure angular coordinates, anatomy-constrained angular coordinates give a meaningful parameterization of the cortical surface in relation to its folding patterns and to the primary developmental, architectonic, functional, and connective axes of the cortex.²

2. Methods and results

2.1. Overview

We have introduced a theoretical framework for the construction of a basic model of the anatomical organization of the cortical surface. Here we present the methods for the construction of the geometric model, the geometric model itself, and finally we propose a set of methods that allows us to use the geometric model as a deformable atlas of the cortical surface. Fig. 2 shows the relations between the concepts and the methods introduced. For the three main aspects of the cortical surface that we consider—homogeneous surface, organizing principal sulci, latter developing

secondary and tertiary sulci—we construct a geometric model defined as a spherical surface with explicitly defined axes and induced folding orientation field (Section 2.4). The structure of the axes of the model is based on the mapping of primary sulci from reconstructed cortical surfaces (Sections 2.2 and 2.3).

In order to use the geometric model as a deformable atlas (Toga and Thompson, 2001) we need to create a bijection between the model and a given reconstructed surface. Here we provide a method based on the numeric solution of a set of PDEs that allows a bijection between any topologically spheric surface and a sphere to be established (Sections 2.5 and 2.6). The axes of the geometric model are then manually adjusted to the corresponding landmarks in the reconstructed surface based on the mapping of primary sulci. The adapted axes are used as boundary conditions for the PDEs to create an anatomy constrained bijection between the cortex and the model (Section 2.7). This defines an anatomy-constrained angular coordinate system for the reconstructed surface, and allows us to obtain for any point a set of anatomy-relative distances, and two folding pattern orientation vectors (Section 2.8) that provide an informative parameterization of the cortical surface.

2.2. Surface reconstruction

We obtain cortical surface reconstructions from anatomical MR images (124 slices, T1-weighted (see also Dale et al., 1999; Dickson et al., 2001)). The white matter is selected by thresholding and is then filtered by a 3D Dynamic Shape algorithm (Koenderink and van Doorn, 1986). Mathematical morphology techniques are used to isolate the cortical white matter inside a hemisphere (Mangin et al., 1995; Dale et al., 1999).

A reconstruction of the cortical surface topologically equivalent to a sphere is then obtained by a hybrid algorithm between deformable surfaces (Kaas et al., 1996; Cohen and Cohen, 1993; Terzopoulos and McInerney, 1996) and voxelization techniques (Kaufman et al., 1993). In the classical deformable surface model the evolution of each vertex v_i is governed by

$$v_i^{t+1} - v_i^t = k_0 F_{int} + k_1 F_{ext} \quad (1)$$

where the external forces F_{ext} drive the surface to the object's boundary (usually a balloon force normal to the surface and a boundary-dependent energy functional (Cohen and Cohen, 1993; McInerney and Terzopoulos, 1996; Xu et al., 1997; Pham et al., 2000)), and the internal forces F_{int} ensure the smoothness of the surface (usually by fixing elasticity and rigidity constraints). The external forces are not able to handle self-collisions, and given this definition, the only means to avoid self-intersections of the surface is to

² The source code used for the construction of the geometric model and atlas can be freely obtained at <http://www.snv.jussieu.fr/insermu483/geometricatlas/index.html>.

use as a starting point a surface very close to the solution or to impose strong smoothness constraints (Xu et al., 1997; Pham et al., 2000). In the deformable hybrid surface the surface mesh is complemented by its voxelization. The external forces are then computed from the voxelized object, which enables us to handle self-collisions while avoiding the use of strong smooth constraints. Unlike classical deformable surfaces, the hybrid surface can expand many times its initial size, and it is able to reconstruct the cortical surface (up to 150.000 vertices) beginning from a single voxel and a cubic mesh (8 vertices). In order to keep a good triangle resolution, the surface is dynamically retriangulated (Schroeder et al., 1992). By labeling the inside of the surface in the voxel volume at each iteration, we override the convergence problem of deformable surfaces, and we avoid using strong smoothing and inflating forces. We start the reconstruction from a one-voxel cubic deformable surface (8 points, 12 triangles) inside the white matter, and expand this surface in its normal direction while dynamically retriangulating it. Fig. 3 illustrates the reconstruction of the white matter.

2.3. Detection and representation of primary sulci

The reconstructed surface is analyzed and deformed to visualize the primary sulcal patterns. The usual mean-curvature mapping does not allow an easy hierarchical distinction of primary, secondary, and tertiary sulci. We use two complementary mappings of the cortical anatomy to detect primary sulci: the sulcal depth and the integrated curvature patterns. These mappings have been used for the construction of the geometric model, and are also used during the manual adaptation of the geometric model to cortical surfaces.

2.3.1. Sulcal depth

The sulcal depth is estimated as the distance from each vertex in the surface to a bounding ellipsoid (the smallest ellipsoid containing the whole reconstructed surface). This distance is evaluated as the resizing factor necessary to obtain the intersection between the vertices and the bounding ellipsoid. We compute k_i , the result of introducing the i -th vertex of coordinates (x_i, y_i, z_i) in the equation of the bounding ellipsoid of semiaxes a, b, c along the x, y, z axes, respectively,

$$\left(\frac{x_i}{a}\right)^2 + \left(\frac{y_i}{b}\right)^2 + \left(\frac{z_i}{c}\right)^2 = k_i. \quad (2)$$

Next we resize the semiaxes of the ellipsoid by a factor d ,

$$\left(\frac{x}{da}\right)^2 + \left(\frac{y}{db}\right)^2 + \left(\frac{z}{dc}\right)^2 = 1. \quad (3)$$

Solving for d_i , we obtain the sulcal depth at this vertex:

$$d_i = \sqrt{k_i} \quad (4)$$

2.3.2. Integrated curvature patterns

The curvature patterns are obtained by integrating the local mean curvature along successive steps of smoothing. Iterative smoothing produces the fading of structures from less to more pronounced, and so the integrated mean curvature gives different weights to primary, secondary, and tertiary sulci.

The smoothing algorithm changes the position of each vertex p_i toward the barycenter of its neighbors. At the smoothing step $t + 1$, the vertex p_i is defined in function of its N_i neighbor points $V_j(p_i)$ as

$$p_i^{t+1} = \frac{1}{N_i} \sum_j V_j(p_i^t). \quad (5)$$

The mean curvature is calculated over the surface at each step. By definition, the mean curvature of a point over a two times differentiable surface is the average of the two principal curvatures k_1 and k_2 in this point (Do Carmo, 1976). We obtain an estimation of the mean curvature at the vertex p_i by calculating a weighted average of the directional curvatures with its neighbors $V_j(p_i)$ in its tangent plane of normal \hat{n} . The directional curvature can be approximated as (Taubin, 1995)

$$\tilde{k}_{ij} = 2\hat{n} \frac{p_i - V_j(p_i)}{\|p_i - V_j(p_i)\|}. \quad (6)$$

The mean curvature K_i at the i -th vertex is then calculated as

$$K_i = \frac{1}{4\pi} \sum_j (\phi_- + \phi_+) \tilde{k}_{ij}, \quad (7)$$

where ϕ_- and ϕ_+ are the angles adjacent to the edge $(p_i, V_j(p_i))$ at the point p_i . The integral of the curvature at the i -th vertex at the smoothing step $t + 1$ is then obtained from

$$c_i^{t+1} = \sum_t f(t) K_i^t, \quad (8)$$

where $f(t)$ allows us to give a stronger weight to the weaker values of the curvature as the smoothing progresses. We usually set $f(t) = 1 + t/T$, with $T \approx 0.5 \times$ the number of iterations.

The integration of the curvature patterns is similar to the mapping of the convexity in Fischl et al. (1999b) or to the mapping of the sulcal roots in Cachia et al. (2001, 2003).

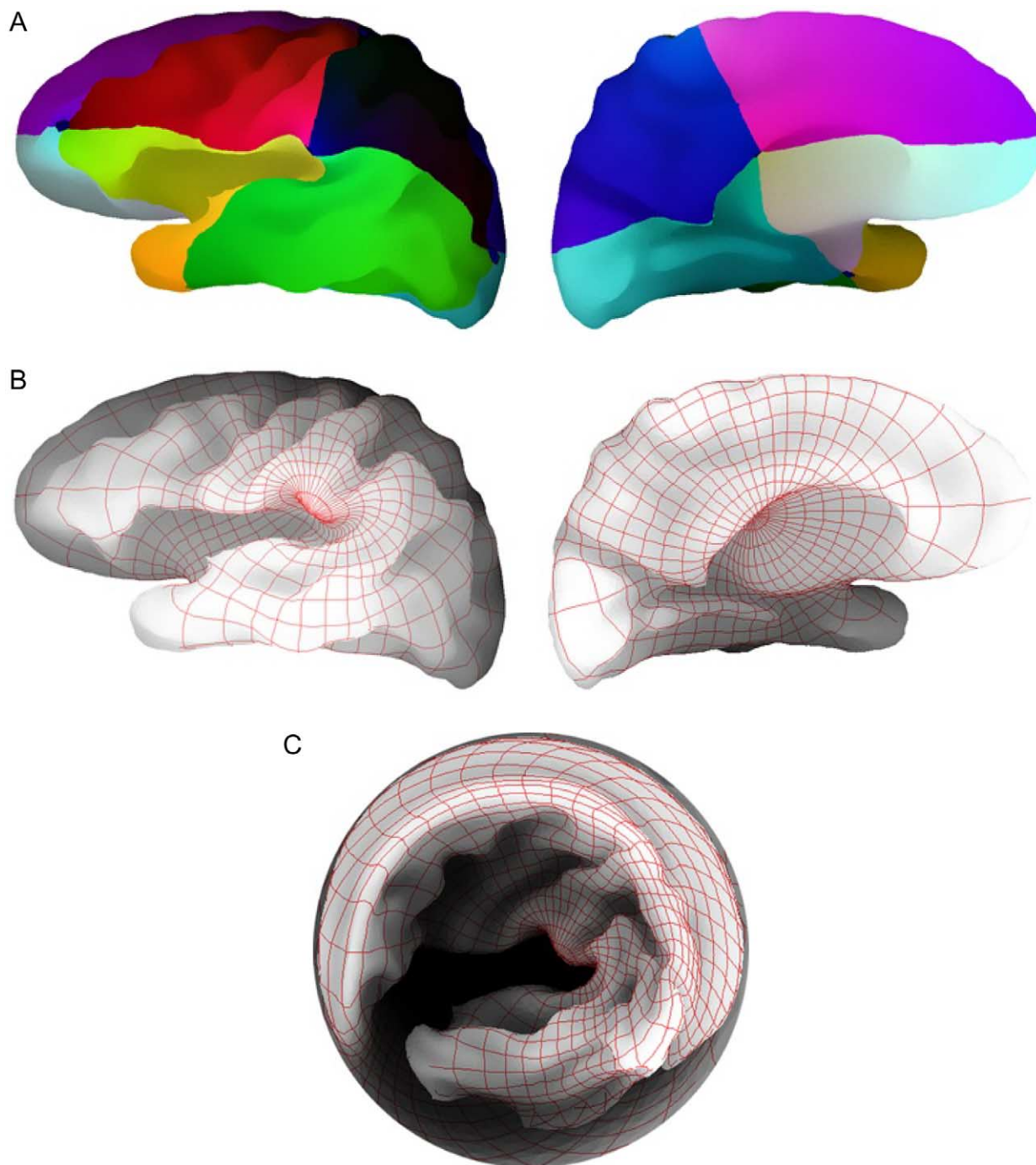


Fig. 7. Bijection between a reconstructed surface and the unitary sphere. The bijection between the reconstructed surface and the unitary sphere is constructed by solving the same set of PDEs over both surfaces, and relating them by the solution of these equations. From top to bottom: (A) temporal and medial views of the solution of the PDEs over the reconstructed surface (X coordinate solution in red, Y coordinate solution in blue, and Z coordinate solution in green), (B) drawing of the spherical coordinates lines, and (C) stereographic representation of the coordinates over the reconstructed surface. Note that while the bijection effectively parameterizes the surface in 2D, there is no a priori correspondence between coordinate lines and sulcal anatomy.

Contrary to Fischl et al. (1999b) what is integrated is not the surface displacement but the mean curvature, which is closely related to the position of gyral crowns and sulcal fundi. The mean curvature is also used in Cachia et al. (2001, 2003), but there, the mesh remains unchanged while

the mean curvature is iteratively smoothed. The resulting mapping is rather different, and where the method of Cachia et al. produces the division of principal sulci into elementary units, the integrated curvature patterns produce continuous sulci.

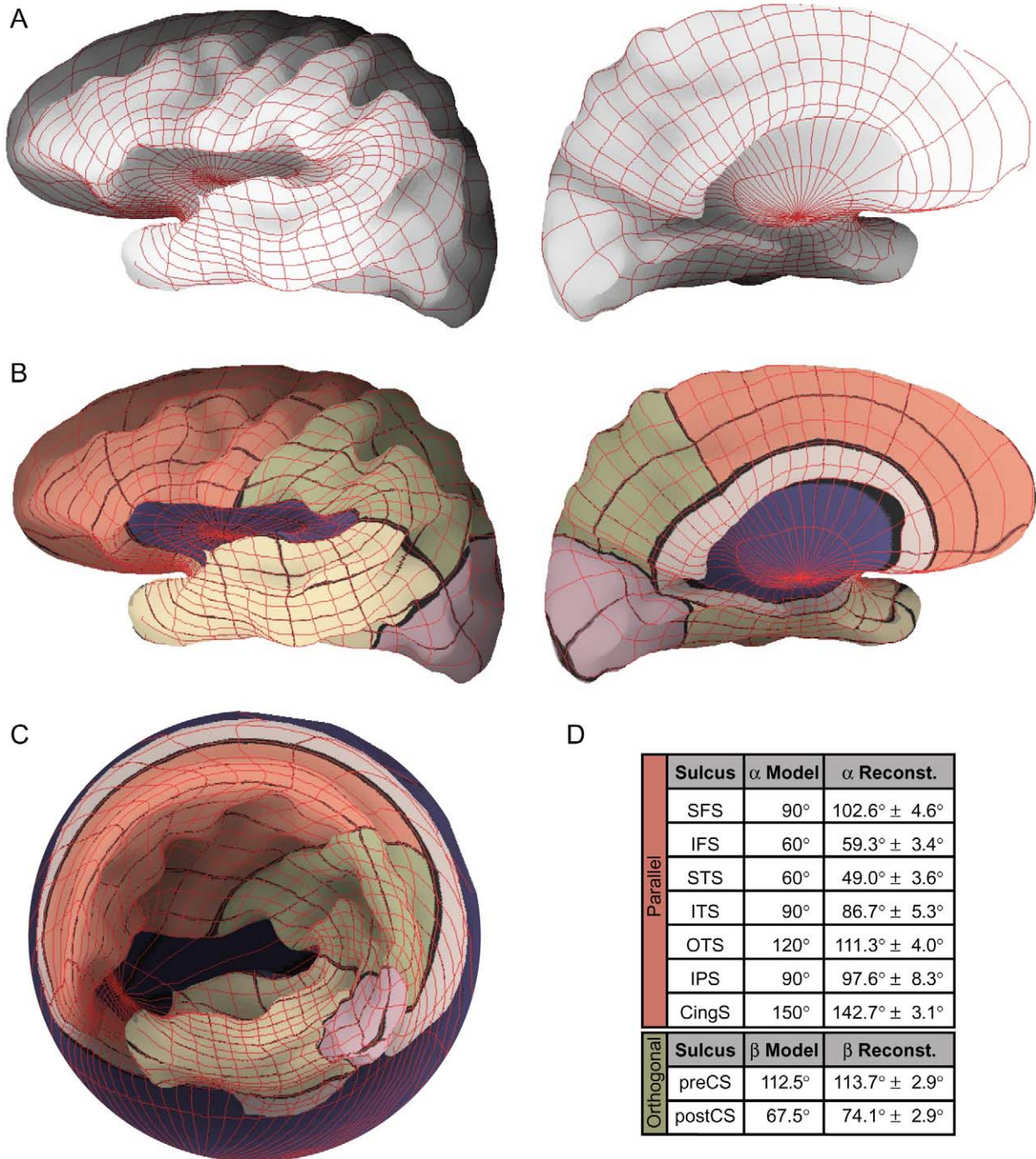


Fig. 8. Constrained bijection between a reconstructed surface and the geometric model. The axes of the geometric model are adapted to the cortical anatomy and a bijection between both surfaces is obtained. By this bijection, the geometric model provides a coordinate system and a folding pattern orientation field for the reconstructed surface. From top to bottom: (A) temporal and medial images of the anatomy-constrained coordinate system, (B) of the geometric model mapped over the cortical surface, and (C) over a stereographic representation. Table D shows the relation between different sulci (not belonging to the axes) and their associated coordinate line (see the text for description). Note that, unlike Fig. 7, the coordinate system lines match the sulcal anatomy.

2.3.3. Representations and stereographic projection

We deform the shape of the initial reconstruction to have a better representation of the sulcal patterns. Sulcal depth and integrated curvature patterns are mapped over reconstructed, smoothed, and spherical models of the cortical surface (Dale and Sereno, 1993; Van Essen and Drury,

1997; Van Essen et al., 1998). We can render for each of these representations a polar stereographic projection (Maling, 1992) that allows us to visualize the whole cortical surface in one image. This projection allows the representation of all the points in the surface but one, and while sizes are not preserved, it preserves shapes and angles. The depth

of the stereographic projection at a given vertex depends on its distance to the center of the mesh. The projection is illustrated for a sphere in Fig. 4.

For each vertex $p_i = (x_i, y_i, z_i)$ of the surface, the cartesian coordinates (a_i, b_i, c_i) in the polar stereographic projection are given by

$$(a_i, b_i, c_i) = \left(\frac{x_i}{\|p_i\|} n_i, \frac{y_i}{\|p_i\|} n_i, \|p_i\| \right), \quad (9)$$

where

$$n_i = \begin{cases} \frac{\theta_i}{\sin \theta_i} & \text{if } \theta_i > 0 \\ 1 & \text{otherwise} \end{cases}$$

$$\theta_i = \arccos \left(\frac{z_i}{\|p_i\|} \right). \quad (10)$$

The metric distortion of the projection is given by $\theta/\sin(\theta)$, so while there is little distortion at the center of the projection (where $\sin(\theta) \approx \theta$), it augments toward the periphery when $\theta \rightarrow \pi$ (that actually represents a single point). Yet, as little computational cost is necessary to obtain a projection, the center can be interactively displaced to diminish the distortion.

Images of the primary sulci from a reconstructed surface are shown in Fig. 5. This figure shows the sulcal depth relative to the bounding ellipsoid and the integration of the mean curvature through successive smoothing steps over the reconstructed, smoothed, and spherical surfaces with its corresponding polar stereographic projections. With a minimal computational cost, the sulcal depth mapping gives a sufficiently accurate hierarchical representation of the cortical surface. The mapping of the integrated curvature patterns, unlike the surface depth mapping, does not depend on the determination of a reference surface (the bounding ellipsoid) for the estimation of the primary sulci. Nevertheless, it gives a vision of gyri and sulci, but not of regions as does the first. We consider both methods as complementary.

2.4. Geometric definition of the model, its axes and folding pattern orientation field

2.4.1. Spherical surface

The geometric model is defined over a sphere that represents the global topological structure of the cerebral cortex of a hemisphere. The hemisphere is artificially closed from the corpus callosum to the hippocampus.

2.4.2. Axes

The axes of the model are a simplification of the primary sulci of the cortical surface as they can be seen from sulcal depth and integrated curvature representations. The most evident anatomical landmarks of the human brain, the insula and the interhemispheric fissure, are easily distinguishable in both representations (Fig. 5). In the sulcal depth repre-

sentation, the insula (IN) is particularly visible as a deep zone at the center of the stereographic projection. In the integrated curvature representation we can observe that the insula is well delimited by the sulci underlying the superior and inferior opercula, and the cingulate sulcus (CingS) that runs parallel to the callosomarginal sulcus (CalmS) at the superior half of the stereographic projection. At the inferior half, the collateral sulcus (CollS) runs parallel to the limit of the cortex. In the geometric model these landmarks, which are also the first visible landmarks in the developing human brain, are chosen as axes of the representation. We further include the Sylvian fissure (SF), central sulcus (CS), calcarine sulcus (CalcS), and lateral occipital sulcus (latOS) that, together with the previously defined axes, divide the geometric model into seven regions: the regions of the frontal lobe (F), parietal (P), occipital (O), temporal (T), insular (IN), limbic (L), and the noncortical region of the artificial closure. These sulci reflect the fissures of the human cortex at approximately 24 weeks of gestation (Feess-Higgins and Larroche, 1987). The area of the regions in the geometric model approximates the measures obtained from cortical surface reconstructions.

2.4.3. Folding pattern orientation field

The orientation field of the geometric model is defined by the geodesic circles orthogonal to the callosomarginal sulcus and the insula, and by the small circles concentric to the insula and the callosomarginal sulcus. This set of curves parallel and orthogonal to the insular and callosomarginal axes provides a natural system of angular coordinates for the cortical surface. In the representation, the distance between curves is chosen to agree with the size and number of cortical convolutions. Fig. 6 shows the resulting folding pattern orientation field of the geometric model with the name of certain sulci overlaid.

2.5. Bijection between two surfaces

In order to use the geometric model as geometric atlas for the analysis of reconstructed cortical surfaces, we need to create a bijection between model and reconstruction. Here we show how to construct such a bijection by solving the Laplace equation over their surfaces. The Laplace equation is frequently used for the definition of coordinates over two dimensional domains (Thompson, 1985; Angenent et al., 1999; Haker et al., 2000), because it presents many advantageous properties: Coordinates generated by the Laplace equation are inherently smooth; they verify the extremum principle (i.e., there cannot be extrema solutions within the domain) which guarantees a one-to-one mapping; discontinuities on the boundary conditions do not propagate into the domain; and finally the coordinate density adjusts itself to the geometry of the domain.

The first step is to generate three smoothly varying parameters between three pairs of antipodal points that will allow a two-dimensional coordinate system to be obtained

for both surfaces. For each parameter $u(p_i)$, we solve the Laplace equation

$$\Delta u = 0 \quad (11)$$

with Dirichlet boundary conditions $(u(\hat{p}), u(\check{p})) = (+1, -1)$ at the two antipodal points \hat{p} and \check{p} (the details of the numerical solution of the equation and the determination of the three pairs of antipodal points are given in the Appendix).

2.6. Bijection between the cortex and the unitary sphere

Over the sphere the antipodal points are simply the maximum and minimum poles at the X , Y , and Z axes; and for any pair of antipodes the solution of the Laplace equation is the same. We obtain a numeric approximation of the function $l = L(x)$; with $l, x \in [-1, 1]$ that gives for a cartesian coordinate x of the unitary sphere, its corresponding Laplace coordinate l . As $l = L(x)$ is a bijection, we can compute the inverse function $x = L^{-1}(l)$ to obtain the cartesian coordinate x of the sphere corresponding to the Laplace coordinate l . Thus, for an arbitrary surface reconstruction of the cortex, the function L allows us to obtain for the three Laplace coordinates (l_x, l_y, l_z) of a point its corresponding cartesian coordinates over the unitary sphere. It is now very simple to deform the reconstructed surface into a sphere: for every point p_i over the reconstruction with laplace coordinates (l_x, l_y, l_z) , we set its cartesian coordinates to $p_i = (L^{-1}(l_x), L^{-1}(l_y), L^{-1}(l_z))$.

The result of the bijection between a reconstructed cortical surface and the unitary sphere is illustrated in Fig. 7. At this point we only have a two-dimensional parameterization of the cortical surface. The next step is to adapt this parameterization to the anatomy of the cortex through the axes of the geometric model.

2.7. Constrained bijection between the cortex and the geometric model

The bijection between the geometric model and a reconstructed cortical surface is created by adjusting the axes in the model to the corresponding landmarks in the reconstruction. The sulcal depth and the integrated patterns of curvature are used to identify primary sulci over the reconstructed surface deformed into a sphere (cf. 2.6). The geometric model and the spheric cortical surface are then represented in a same stereographic projection. We have developed an interface to interactively rotate the stereographic projection by dragging it, and manually adjust the superimposed geometric model by acting over the control points of its axes defined as spherical Bézier curves. The correctness of the adjustment can be verified over the nondeformed reconstructed surface.

The adjusted axes of the geometric model are then used to set up boundary conditions for the solution of the Laplace

equations over the reconstructed cortex. The equations are solved over a modified spherical mesh that has vertices underlying the adjusted axes. At these vertices we set Dirichlet conditions to the value of the solution of the Laplace equations over the sphere of the geometric model. The final bijection between the reconstructed surface and the model is interpolated from this modified mesh. Fig. 8 shows the result of the constrained bijection.

Contrary to the unconstrained bijection (cf 2.6), the coordinate lines of the constrained bijection globally follow the two principal orientations of the cortical folding patterns, providing what we call an *anatomy-constrained angular coordinates* system for the cortical surface. Table D in Fig. 8 shows the relation between different sulci (not belonging to the axes) and the coordinate lines of the folding pattern field. The fundi of the sulci in the table have been manually traced over a reconstructed cortical surface and its average coordinate and standard deviation calculated. The average anatomy-constrained angular coordinate of sulci can be compared to the coordinate assigned by the geometric model (Table D, α coordinate for parallel sulci, β coordinate for orthogonal sulci).

2.8. Anatomy-relative distances and folding pattern orientation vectors

The explicit definition of the principal anatomical landmarks, represented by the axes of the geometric model, enables us to obtain for any point of the surface (except the poles $\alpha = 0, \alpha = \pi$) a set of a *anatomy-relative distances*. They measure the surface distance between a point and the axes of the geometric model along the lines of the anatomy-constrained coordinate system. The distance is numerically integrated over the reconstructed cortical surface following a coordinate line defined over the geometric model.

The model for the orientation of the cortical folding patterns provided by the folding pattern orientation field allows us to obtain, for any point of the surface except the poles, two vectors that locally indicate its principal folding orientations, the *folding pattern orientation vectors*. Over the geometric model, the lines of the folding pattern orientation parallel to the insula form a set of small circles with the center over the z -axis, while the orthogonal lines follow the geodesics circles whose plane's normal is orthogonal to the z -axis. For a point of anatomy-constrained angular coordinates (α, β) , the parallel and orthogonal orientation vectors F_p, F_o are given over the geometric model by

$$F_p = (-\sin(\alpha)\sin(\beta), \sin(\alpha)\cos(\beta), 0) \quad (12)$$

$$F_o = (\cos(\alpha)\cos(\beta), \cos(\alpha)\sin(\beta), -\sin(\alpha)). \quad (13)$$

Over the reconstructed surface, these vectors are approximated as the tangent to the anatomy-constrained coordinate lines for the point. The approximation is obtained by a simple centered finite difference. Fig. 9 shows the anatomy-

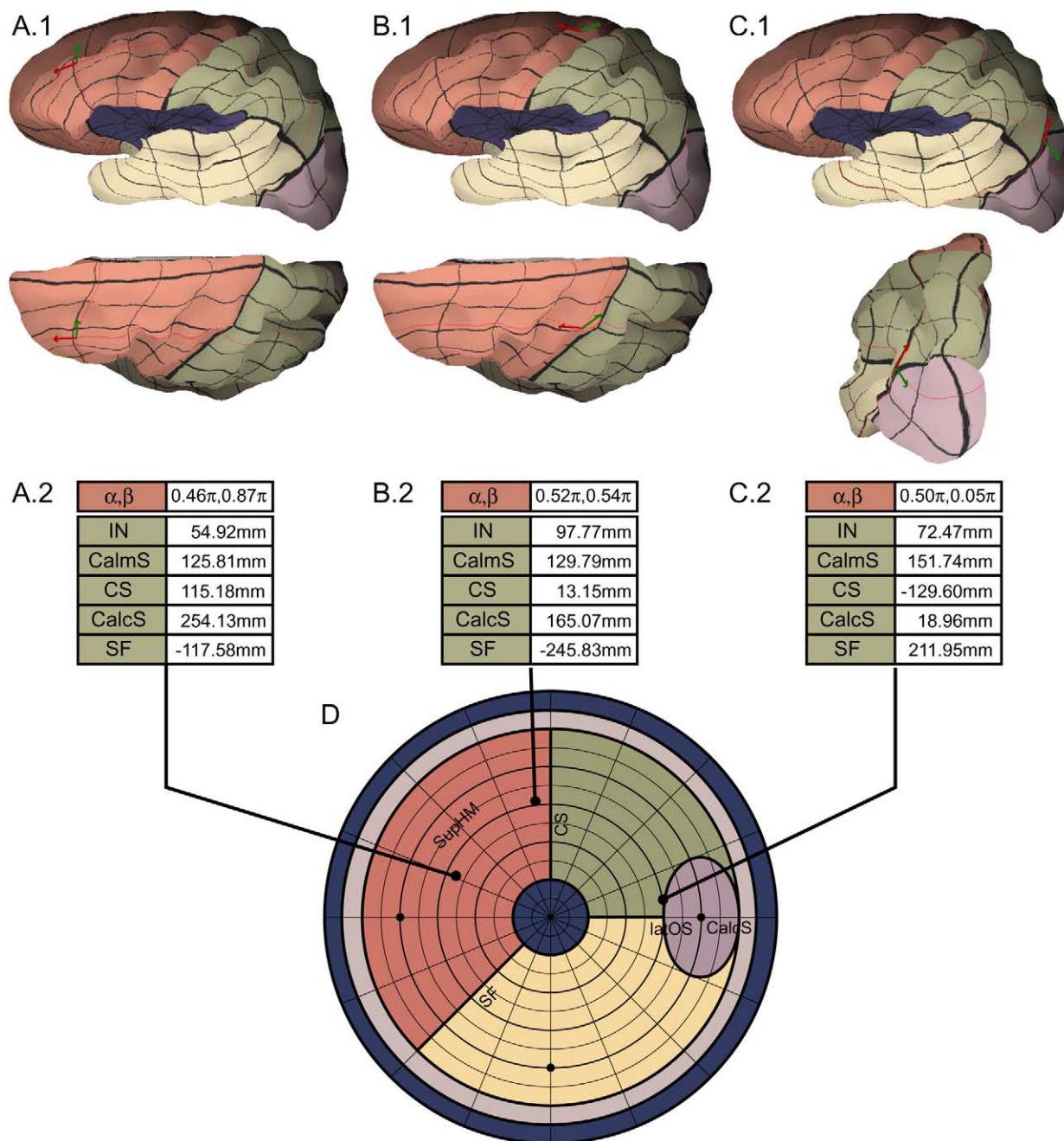


Fig. 9. Anatomy-constrained coordinates, anatomy-relative distances, and folding pattern orientation vectors. The parameters are given for three different points over the cortical surface. The paths over the surface used to compute the anatomy-relative distances are drawn in red; the parallel and orthogonal folding orientation vectors are drawn in green and red, respectively. Top row from left to right: temporal and parietal views of (A.1) a point on the intermediate frontal gyrus, (B.1) a point on the precentral gyrus, and (C.1) a point over the lateral occipital sulcus. Middle row from left to right: (A.2, B.2, C.2) corresponding anatomy-constrained angular coordinates and anatomy-relative distances. (D) Location of the points over a stereographic representation of the geometric model.

relative distances and folding pattern orientation vectors for three points over the cortical surface.

3. Discussion

Sulci and gyri are playing an increasingly important role in functional neuroimaging. For a variety of cognitive pro-

cesses, functional activity is found to be associated to a particular sulcus or gyrus, and not just confined to a given Brodmann area.

Recent surface-based atlases avoid an explicit definition of gyri and sulci, which simplifies the automatization of morphing in databases. Fischl et al. (1999b), for example, replace the explicit definition of the sulcal anatomy by a

label of the local convexity over the surface. A correspondence between this surface and an average labeled surface is then obtained by trying to keep a balance between the minimization of disparity and the local metric distortion. In this way it is possible to reparameterize any surface into a common coordinate system, but without any information concerning distances to main sulci, or the orientation of the folding pattern at any point. To obtain it, an explicit definition of the sulcal anatomy is necessary, where the anatomy is not just labeled, but where its form is detected.

The explicit definition of a particular anatomical structure has been successfully used to measure its variability inside a population. For example, Thompson et al. (1996) have used a set of manually traced sulci to evaluate variations of the cortical anatomy. This allows us to precisely compare among individual structures of the cerebral cortex. Yet, the approach does not make explicit a global organization for the set of locally defined sulci, and the descriptions remain unconnected.

In our present work we have introduced a geometric model of the cortical surface that explicitly includes principal sulci and other important anatomical landmarks in a global model for the orientation of its folding patterns. The geometric model addresses two fundamental aspects of the cortical anatomy: the two-dimensional character of its layered structure; and its architectonic, connectional, and functional differentiation in gyri and sulci. While much is known about the ontogenesis of the cortical layered structure, the mechanisms underlying gyrogenesis remain poorly understood. In consequence, the geometric model only tries to capture the more basic traits of the cortical folding patterns. Further studying the mechanisms of cortical development should permit, for example, a deeper understanding of the relations between primary and secondary sulci that the geometric model can only suggest based on mainly qualitative considerations.

We have introduced new representations of the cortical anatomy intended to simplify the visualization of the principal sulci and other anatomical landmarks that serve as axes of the geometric model. The mapping of the sulcal depth and the integrated curvature patterns use the differences in the structure of principal sulci to distinguish them from secondary and tertiary sulci. The polar stereographic projections facilitate the inspection of the whole cortical surface, from any point of view, without need of artificial cuts, and as fast as a normal render—unlike fixed viewpoint and time-consuming flat maps (Van Essen and Drury, 1997; Van Essen et al., 1998; Fischl et al., 1999a).

We have presented a new method that allows us to adapt the surface and the folding pattern of the geometric model to a reconstructed cortical surface. The geometric model can be then used as a two-dimensional coordinate system, folding orientation field and deformable atlas. The adaptation is based on a general procedure to establish a two-dimensional coordinate system over topologically spheric surfaces. A first parameterization in angular coordinates is obtained by

solving a set of PDEs directly over the reconstructed surface mesh, avoiding the previous step of spherical deformation required by most of the current surface-based approaches (Van Essen and Drury, 1997; Van Essen et al., 1998; Fischl et al., 1999a). Then, the adaptation of the folding pattern is obtained by using the axes of the geometric model (manually adjusted to its corresponding cortical landmarks) as boundary conditions for the set of PDEs. This produces an anatomy-constrained angular coordinates system, where the coordinate lines are related to the principal folding directions of the cortex. The anatomy-constrained angular coordinates provide new means for the characterization of the cerebral cortex in relation to its main organizing landmarks (through the anatomy-relative distances) and folding pattern orientation (through the folding pattern orientation vectors).

The geometric atlas makes two hypotheses concerning the organization of the cortical surface: that a set axes induce a folding pattern field, and that remaining sulci are oriented along this field. Only the set of axes is strictly matched between the geometric atlas and reconstructed cortices. How precisely is then matched the same sulcus among different cortices when the sulcus does not belong to the axes? While it should seem natural to respond by increasing the number of sulci in the axes set, registering different cortices based on matching every sulci is a controversial strategy. Indeed, a relation between sulcal anatomy and cortical architecture or function seems clear at present only for some primary sulci (Zilles et al., 1997; Roland and Zilles, 1998; Morosan et al., 2001; Hasnain et al., 2001). Furthermore, it is possible that even if a cytoarchitectonic (or functional) border does not match a specific gyri or sulci, it can follow the local orientation of the folding pattern field (e.g., borders in the somatosensory cortex are oriented along the postcentral gyrus). The validation of the geometric atlas involves then two complementary aspects: how well sulci are related to the directions of the folding pattern field, and how well cytoarchitectonically or functionally stable sulci are related to a particular coordinate line. This validation might lead to the introduction of new axes to the geometric model only if this improves the global matching of the folding pattern and if the new axes are stable. In order to simplify the validation of the geometric model and the adaptation method against a database of cortices it seems important to introduce an automatic strategy of sulcal detection, such as those proposed by Rivière et al. (2002) and Tao et al. (2002), which should also improve the adaptation method.

The restriction of the analysis of functional activity to the cortical surface has been shown to improve the statistical power of statistical parametric maps when compared to the classical three-dimensional analysis in Talairach coordinates (Fischl et al., 1999b). Equivalently, in regards to the role of gyri and sulci in the organization of the cerebral cortex, it is reasonable to expect that an anisotropic analysis of functional activity directed by the principal orientations of the folding pattern will further improve the detection of

functional activity. However, beyond a possible enhancement of the detection of activity, we believe that the major contribution of our present work is the proposition of a theoretical framework for the study of the anatomical organization of the cortical surface, on which further modeling, representation, and mapping are based. It is an initial step, and a first tool, for investigating the relationship between the fundamental processes of convolution development and the final adult structure and function of the human cerebral cortex.

Acknowledgments

We thank E. Carey, L. Garnero, J.-P. Aubin, and O. Faugeras for helpful reading of the original manuscripts. R.T. has been supported in part by Scito S.A. and the Ecos/Conycit Committee.

Appendix

Bijection between two surfaces

We solve numerically the Laplace equation over each surface

$$\Delta u = 0 \quad (\text{A.1})$$

with three pairs of antipodal poles set as Dirichlet conditions of values $+1$ and -1 . The solution is obtained by the finite element method (Hughes, 1987), that we will briefly outline.

To approximate the solution of the Laplace equation over a surface Ω composed of triangular finite elements, we first construct a *weak formulation* for the problem,

$$\iint_{\Omega} \Delta u f dS = 0, \quad (\text{A.2})$$

where the function f is composed of piecewise linear functions ϕ_p that for each vertex p, q of the mesh satisfy $\phi_p(q) = \delta_{pq}$ ($\delta_{ij} = 1$ iff $i = j$ is the Dirac symbol). Integrating by parts we obtain that (A.2) is equivalent to

$$\iint_{\Omega} \nabla u \nabla f dS = 0. \quad (\text{A.3})$$

Next, the same piecewise linear functions ϕ_p are used to interpolate the solution u as

$$u \approx \sum_p u_p \phi_p \quad (\text{A.4})$$

so we need to solve the set of linear equations

$$Au = B, \quad (\text{A.5})$$

where

$$A_{pq} = \iint_{\Omega} \nabla \phi_p \nabla \phi_q dS \quad (\text{A.6})$$

with

u = the solution vector

A = the stiffness matrix

B = the boundary condition vector (zero for the homogeneous solution)

The coefficients A_{pq} for a vertex p will only depend on the j vertices $q = V_j(p_i)$ of its neighborhood. For any other q such that q do not belong to the neighborhood, $\phi_p \phi_q = 0$. The coefficients of the matrix A are given by

$$\begin{aligned} A_{pq} &= -\frac{1}{2} (\cot(\phi_-) + \cot(\phi_+)), p \neq q \\ A_{pp} &= -\sum A_{pq}, \end{aligned} \quad (\text{A.7})$$

where ϕ_+, ϕ_- are the angles adjacent to the edge $(p, V_j(p_i))$ at the point p_i .

Now we need to modify the matrices A and B to introduce the Dirichlet boundary conditions. In order to set a Dirichlet condition at the vertex p , i.e., to fix the solution at the vertex p to the value u_0 , we modify $(A, B) \rightarrow (A', B')$ as

$$\begin{aligned} A'_{ip} &= A'_{pi} = \delta_{ip} \\ B'_p &= u_0 \\ B'_q &= B_q + A_{pq} u_0 \end{aligned} \quad (\text{A.8})$$

for $i = 1 \dots N$ and $q \in V_j(p_i)$.

To solve the system of linear equations we use the conjugated gradients method (Press et al., 1992), with an appropriate sparse matrix storage scheme to avoid using the raw N^2 matrix.

When the system (A.5), (A.8) is solved over a sphere with boundary conditions at the poles \hat{p}, \check{p} set to $(u(\hat{p}), u(\check{p})) = (+1, -1)$ the level curve for the value $u = 0$ is a great circle, i.e., a geodesic circle that divides the sphere in two equivalent hemispheres. If \hat{p} and \check{p} are antipodal points the level curves of the solution form a set of parallel small circles. In a general surface, the level curve $u = 0$ will not divide the surface in two equal-area halves, so we have to force the level curve $u = u_h$ to $u_h = 0$. If m and s are the two vertices of an edge (m, s) such that the solution of (A.5) is $u(m) > u_h$ and $u(s) < u_h$, we will have the new problem

$$A''u = B' \quad (\text{A.9})$$

with the new constraints

$$\frac{u(s)}{(1-t)} + \frac{u(m)}{t} = 0 \quad (\text{A.10})$$

where $t = 1 - u_h/(u_m - u_s)$, or equivalently

$$u(s) = au(m) \quad (\text{A.11})$$

where $a = (t - 1)/t$.

To include these new equations we have to change $A' \rightarrow A''$ such that

$$\begin{aligned} A'_{mm} &= A'_{mm} + a^2 A'_{ss} \\ A'_{im} &= A_{mi} = A'_{im} + a A'_{is} \\ A'_{is} &= A'_{si} = \delta_{is} \end{aligned} \quad (\text{A.12})$$

Solving this new linear system we obtain a coordinate that distributes smoothly from one pole to the other.

We create a coordinate system over the surface by applying three times this procedure to obtain the (redundant) surface coordinates u_x , u_y , and u_z . First we choose two preliminary X poles (the most frontal and most occipital point over the surface, for example), and at the $u_x = 0$ level curve we choose a pair of preliminary Z poles (the most temporal and most medial point over the curve, for example). At the intersection of the curves $u_x = 0$ and $u_z = 0$ we obtain the first pair $(+Y, -Y)$ of “antipodal” points (points at the intersection of two great circles). Solving for these antipodal points we obtain two new pairs of antipodal points $(+X, -X)$, $(+Z, -Z)$. The final coordinate system is obtained by solving the PDEs with Dirichlet conditions $(+1, -1)$ at the antipodal points and zero at the corresponding great circles.

As the algorithm calculates a transformation that addresses the surface reconstruction as a topologic sphere (unlike Haker et al., 2000), we obtain a coordinate system for the whole cortical surface instead of only a disk.

References

- Angenent, S., Haker, S., Tannenbaum, A., Kikinis, R., 1999. Laplace-Beltrami operator and brain surface flattening. *IEEE Trans. Med. Imaging* 18, 700–711.
- Armstrong, E., Schleicher, A., Omran, H., Curtis, M., Zilles, K., 1995. The ontogeny of human gyrification. *Cereb. Cortex* 1, 56–63.
- Bailey, P., von Bonin, G., 1950. *The Isocortex of Man*. Univ. of Illinois Press, Champaign.
- Cachia, A., Mangin, J., Rivière, D., Boddaert, N., Andrade, A., Kherif, F., Sonigo, P., Papadopoulos-Orfanos, D., Zilbovicius, M., Poline, J., Bloch, I., Brunelle, F. and Régis, J., 2001. A mean curvature based primal sketch to study the cortical folding process from antenatal to adult brain, in: *Proc 4th MICCAI, Utrecht, The Netherlands, 2001*, Springer-Verlag, Berlin, pp. 897–904.
- Cachia, A., Mangin, J., Rivière, D., Kherif, F., Boddaert, N., Andrade, A., Papadopoulos-Orfanos, D., Poline, J., Bloch, I., Zilbovicius, M., Sonigo, P., Brunelle, F., Régis, J. 2003. A primal sketch of the cortex mean curvature: a morphogenesis based approach to study the variability of the folding patterns. In press.
- Chung, M., 2001. *Statistical Morphometry in Neuroanatomy*. Ph.D. thesis. McGill University, Montreal.
- Cohen, L., Cohen, I., 1993. Finite-element methods for active contour models and balloons for 2-D and 3-D images. *Pattern Anal. Mach. Intell.* 15, 1131–1147.
- Connolly, C., 1950. *External Morphology of the Primate Brain*. Thomas, Springfield, IL.
- Dale, A., Fischl, B., Sereno, M., 1999. Cortical surface-based analysis. I. Segmentation and surface reconstruction. *NeuroImage* 9, 179–194.
- Dale, A., Sereno, M., 1993. Improved localization of cortical activity by combining EEG and MEG with MRI cortical surface reconstruction: a linear approach. *J. Cogn. Neurosci.* 5, 162–176.
- Damasio, H., 1995. *Human Brain Anatomy in Computerized Images*. Oxford University Press, London.
- Dickson, J., Drury, H., Van Essen, D., 2001. ‘The surface management system’ (SuMS) database: a surface-based database to aid cortical surface reconstruction, visualization and analysis. *Philos. Trans. R. Soc. London B.* 356, 1277–1292.
- Do Carmo, M., 1976. *Differential Geometry of Curves and Surfaces*. Prentice-Hall, Englewood Cliffs, NJ.
- Feess-Higgins, A., Larroche, J., 1987. *Development of the Human Foetal Brain*. Inserm-Masson, Paris.
- Fischl, B., Sereno, M., Dale, A., 1999a. Cortical surface-based analysis. II. Inflation, flattening, a surface-based coordinate system. *NeuroImage* 9, 195–207.
- Fischl, B., Sereno, M., Tootell, R., Dale, A., 1999b. High-resolution intersubject averaging and a coordinate system for the cortical surface. *Hum. Brain Mapp.* 8, 272–284.
- Goldman, P., Galkin, T., 1978. Prenatal removal of frontal association cortex in the fetal rhesus monkey: anatomical and functional consequences in postnatal life. *Brain Res.* 152, 451–485.
- Goldman, P., Nauta, W., 1977. Columnar distribution of cortico-cortical fibers in the frontal association, limbic, and motor cortex of the developing rhesus monkey. *Brain Res.* 122, 393–413.
- Goldman-Rakic, P., 1980. Morphological consequences of prenatal injury to the primate brain. *Prog. Brain Res.* 53, 3–19.
- Haker, S., Angenent, S., Tannenbaum, R., Kikinis, R., Sapiro, G., Halle, M., 2000. Conformal surface parameterization for texture mapping. *IEEE Trans. Visual. Comput. Graphics* 6, 181–189.
- Hasnain, M., Fox, P., Woldorff, M., 2001. Structure-function spatial covariance in the human visual cortex. *Cereb. Cortex* 11, 702–716.
- Hubel, D., Wiesel, T., 1977. Functional architecture of macaque monkey visual cortex. *Proc. R. Soc. London B* 198, 1–59.
- Hughes, T., 1987. *The Finite Element Method*. Prentice Hall, Englewood Cliffs, NJ.
- Jacobson, M., 1991. *Developmental Neurobiology*, third ed. Plenum, New York.
- Kaas, M., Witkin, A. and Terzopoulos, D., 1996. Snakes: active contour models, in: *International Conference on Computer Vision*, pp. 259–269.
- Kaufman, A., Cohen, D., Yagel, R., 1993. Volume graphics. *IEEE Comp.* 26, 51–64.
- Koenderink, J., van Doorn, A., 1986. Dynamic shape. *Biol. Cybern.* 53, 383–396.
- Malamud, N., Hirano, A., 1974. *Atlas of Neuropathology*, second rev. ed. Univ. of California Press, Berkeley.
- Maling, D., 1992. *Coordinate Systems and Map Projections*, second ed. Pergamon, Elmsford, NY.
- Mangin, J., Bloch, I., Régis, J., López-Krahe, J., 1995. From 3D magnetic resonance images to structural representations of the cortex topography using topology preserving deformations. *J. Math. Imaging Vision* 5, 297–318.
- Marin-Padilla, M., 1988. Early ontogenesis of the human cerebral cortex, in: Jones, E., Peters, A. (Eds.), *Cerebral Cortex*, Vol. 7. Plenum, New York, pp. 1–30.
- McInerney, T., Terzopoulos, D., 1996. Deformable models in medical image analysis: A survey. *Med. Image Anal.* 1, 91–108.
- Morosan, P., Rademacher, J., Schleicher, A., Amunts, K., Schormann, T., Zilles, K., 2001. Human primary auditory cortex: cytoarchitectonic subdivisions and mapping into a spatial reference system. *NeuroImage* 13, 684–701.
- Mountcastle, V., 1957. Modality and topographic properties of single neurons of cat’s somatic sensory cortex. *J. Neurophysiol.* 20, 408–434.
- Mountcastle, V., 1978. Organizing principle for cerebral function: the unit module and the distributed system, in: Edelman, G., Mountcastle, V. (Eds.), *The Mindful Brain*, MIT Press, Cambridge, MA, pp. 7–50.

- Mountcastle, V., 1997. The columnar organization of the neocortex. *Brain* 120, 701–722.
- Nieuwenhuys, R., ten Donkelaar, H., Nicholson, C., 1997. *The Central Nervous System of Vertebrates*. Springer-Verlag, Berlin.
- Ono, M., Kubik, S., Abernathy, C., 1990. *Atlas of the Cerebral Sulci*. Thieme, New York.
- Pham, D., Xu, C., Prince, J., 2000. Current methods in medical image segmentation. *Annu. Rev. Biomed. Eng.* 2, 315–337.
- Press, W., Teukolsky, S., Vetterling, W., Flannery, B., 1992. *Numerical Recipes in C (The Art of Scientific Computing)*. Cambridge Univ. Press, Cambridge, UK.
- Rakic, P., 1988. Specification of cerebral cortical areas. *Science* 241, 170–241.
- Régis, J., Mangin, J., Ochiai, T., Frouin, V., Rivière, D., Cachia, A., Do, L. and Samson, Y., 2003. The “Sulcal roots” generic model: a hypothesis to overcome the variability of the human cortex folding patterns. Submitted for publication.
- Rivière, D., Mangin, J., Papadopoulos-Orfanos, D., Martinez, J., Frouin, V., Régis, J., 2002. Automated recognition of cortical sulci of the human brain using a congregation of neural networks. *Med. Image Anal.* 6, 77–92.
- Roland, P., Zilles, K., 1998. Structural divisions and functional fields in the human cerebral cortex. *Brain Res. Rev.* 26, 87–105.
- Schroeder, W., Jonathan, A., Lorensen, W., 1992. Decimation of triangle meshes. *Comput. Graphics* 26 (2), 65–70.
- Smart, I., McSherry, G., 1986a. Gyrus formation in the cerebral cortex in the ferret. I. Description of the external changes. *J. Anat.* 146, 141–152.
- Smart, I., McSherry, G., 1986b. Gyrus formation in the cerebral cortex in the ferret. II. Description of the internal histological changes. *J. Anat.* 147, 27–43.
- Spitzer, V., Ackerman, M., Scherzinger, A., Whitlock, D., 1996. The visible human male: a technical report. *J. Am. Med. Informatics Assoc.* 3, 118–130.
- Talairach, J., Tournoux, P., 1988. *Co-Planar Stereotaxic Atlas of the Human Brain*. Thieme, Stuttgart.
- Tao, X., Prince, J., Davatzikos, C., 2002. Using statistical shape model to extract sulcal curves of the outer cortex of the human brain. *IEEE Trans. Med. Imaging* 21, 513–524.
- Taubin, G., 1995. Estimating the tensor of curvature of a surface from a polyhedral approximation, in: *International Conference on Computer Vision*, pp. 902–907.
- Terzopoulos, D., McInerney, T., 1996. Deformable models in medical image analysis, in: *Proc of MMBIA*, pp. 171–180.
- Thompson, J., 1985. *Numerical Grid Generation*. Elsevier, Amsterdam.
- Thompson, P., MacDonald, D., Mega, M., Holmes, C., Evans, A., Toga, A., 1996. Detection and mapping of abnormal brain structures with a probabilistic atlas of cortical surfaces. *J. Comput. Assist. Tomogr.* 21, 557–581.
- Thompson, P., Toga, A., 1997. Detection, visualization and animation of abnormal anatomic structures with a deformable probabilistic brain atlas based on random vector field transformations. *Med. Image Anal.* 1, 271–294.
- Todd, P., 1982. A geometric model for the cortical folding pattern of simple folded brain. *J. Theor. Biol.* 97, 529–538.
- Todd, P., 1985. Gaussian curvature as a parameter of biological surface growth. *J. Theor. Biol.* 113, 63–68.
- Toga, A., Thompson, P., 2001. Maps of the brain. *Anat. Rec.* 265, 37–53.
- Valverde, F., 1986. Intrinsic neocortical organization: some comparative aspects. *Neuroscience* 18, 1–23.
- Van Essen, D., Drury, H., 1997. Structural and functional analyses of human cerebral cortex using a surface-based atlas. *J. Neurosci.* 17, 7079–7102.
- Van Essen, D., Drury, H., Joshi, S., Miller, M., 1998. Functional and structural mapping of human cerebral cortex: solution are in the surfaces. *Proc. Natl. Acad. Sci. USA* 95, 788–795.
- Welker, W., 1990. Why does cerebral cortex fissure and fold? A review of determinants of gyri and sulci, in: Jones, E., Peters, A. (Eds.), *Cerebral Cortex*, volume 8b. Plenum, New York, pp. 3–136.
- Xu, C., Pham, D., Prince, J., 1997. Finding the brain cortex using fuzzy segmentation, isosurfaces and deformable surface models, in: *International Conference on Information Processing in Medical Imaging*, pp. 399–404.
- Zilles, K., Schleicher, A., Langemann, C., Amunts, K., Morosan, P., Palomero-Gallagher, N., Schormann, T., Mohlberg, H., Burgel, U., Steinmetz, H., Schlaug, G., Roland, P., 1997. Quantitative analysis of sulci in the human cerebral cortex: development, regional heterogeneity, gender difference, asymmetry, intersubject variability and cortical architecture. *Hum. Brain Mapp.* 5, 218–221.